PHYSICS

Single-asperity sliding friction across the superconducting phase transition

Wen Wang[1,2], Dirk Dietzel[1,3]*, André Schirmeisen[1,3]*

In sliding friction, different energy dissipation channels have been proposed, including phonon and electron systems, plastic deformation, and crack formation. However, how energy is coupled into these channels is debated, and especially, the relevance of electronic dissipation remains elusive. Here, we present friction experiments of a single-asperity sliding on a high-T_c superconductor from 40 to 300 kelvin. Overall, friction decreases with temperature as generally expected for nanoscale energy dissipation. However, we also find a large peak around T_c. We model these results by a superposition of phononic and electronic friction, where the electronic energy dissipation vanishes below T_c. In particular, we find that the electronic friction constitutes a constant offset above T_c, which vanishes below T_c with a power law in agreement with Bardeen-Cooper-Schrieffer theory. While current point contact friction models usually neglect such friction contributions, our study shows that electronic and phononic friction contributions can be of equal size.

INTRODUCTION

One of the main challenges to progress in the area of sliding friction is the complex nature of both natural and engineered surfaces, exhibiting surface roughness at different length scales, constituting a multi-asperity contact. Friction force microscopy (FFM) in which a nanometer-sized tip slides on a flat surface can be viewed as a minimalistic model case. A wealth of experimental and theoretical research exists on sliding friction of single-asperity contacts (*1*–*8*).

For a clean, low-wear sliding contact, generally, two mechanisms are believed to contribute to sliding friction: On one hand, friction relates to the excitation of phonons due to the mechanical interaction of tip and surface. In this context, especially discontinuous stick-slip-type asperity movements, as described by the Prandtl-Tomlinson (PT) model (*9*–*11*), are considered responsible for phonon injection into the sample volume. To simplify matters, we refer this friction mechanism to as phononic friction in the following paragraphs.

The term electronic friction (*12*), on the other hand, describes effects where energy dissipation is linked to interaction with the electron system. In this context, a number of different mechanisms have been suggested. Most of them center around the idea that a sliding tip or sliding adsorbates can drive charges through surface atomic layers experiencing electrical resistance, i.e., joules dissipation by effects like scattering and electron hole pair creation (*1*, *12*–*14*). More recently, in addition, energy dissipation mechanisms based on electrostatic interaction due to charge trapping have been suggested (*15*, *16*), while even a link between electronic and phononic effects may exist on the basis of electron-phonon coupling (*17*, *18*). If the material resistivity approaches zero, as is the case for a superconductor below T_c, this electronic friction should vanish as well.

First, experiments explicitly targeting the electronic friction channel measured the damping of a quartz crystal microbalance (QCM) with a solidified nitrogen layer on a lead surface (*19*). A marked drop of energy dissipation appeared below the transition temperature T_c for superconductivity of Pb and was assigned to the decrease in electronic friction of the nitrogen atoms sliding on lead. Later on, measurements from the same group reported an even larger friction drop of 50% for N_2 and He films on superconducting Pb substrate (*20*). Those results have sparked considerable interest into the problems of electronic friction and spurred a number of different theoretical and experimental works later on (*7*, *12*, *13*, *16*, *21*–*24*). More recently, non-contact friction experiments have demonstrated that the damping of an oscillating cantilever decreases strongly when crossing the superconducting phase transition temperature of Nb (*25*). These experiments proved that electronic damping is suppressed by the superconducting phase but the relevance for sliding friction with asperities in contact remains unclear. So far, only one experiment explicitly targeted single-asperity friction on a high-temperature YBCO superconductor (*16*) with a focus on the levitation force using magnetic tips. In addition, here, a significant decrease in friction was found in correlation to the superconducting phase transition.

Among the wealth of current theories applied to single-asperity sliding friction experiments on the nanoscale, none explicitly accounts for electronic friction effects. Usually, it is argued that electronic friction is proportional to velocity, which is several orders of magnitude smaller for FFM experiments than in realistic tribocontacts, where macroscopic experiments already hinted at the potential influence of electronic friction (*26*, *27*). Therefore, it is generally assumed that phonon excitation by the stick-slip-type tip motion for sliding nanocontacts simply dominates over independent electronic friction effects. However, there is no experimental evidence to support this hypothesis. Knowledge about the relative contribution of electronic friction contributions is also highly relevant for the emerging field of superlubricity (*28*), where a structural mismatch between atomically flat interfaces leads to a vanishing corrugation of the periodic energy surface during sliding and electronic friction should dominate. From a more fundamental point of view, especially, the transition regime around the superconducting phase transition must be considered a key element to understand the role of charge carriers in the friction process. A particularly crucial question for comparison with theoretical models is whether electronic friction contributions vanish as soon as the electrical resistance is zero or if the remaining normal-state electrons can still contribute to the dissipation process below T_c.

[1]Institute of Applied Physics (IAP), Justus-Liebig-Universität Giessen, 35392 Giessen, Germany. [2]School of Mechanical Engineering, Southwest Jiaotong University, 610031 Chengdu, China. [3]Center for Materials Research, Justus-Liebig-Universität Giessen, 35392 Giessen, Germany.
*Corresponding author. Email: andre.schirmeisen@ap.physik.uni-giessen.de (A.S.); dirk.dietzel@ap.physik.uni-giessen.de (D.D.)

Here, we report sliding friction experiments with a silicon nanotip on a high-T_c bismuth strontium calcium copper oxide (BSCCO) superconductor as a function of temperature. Above T_c, friction decreases with temperature in agreement with the thermally activated PT model (*6*, *10*). Upon cooling below T_c, however, we find a drop of approximately 30% in friction, which can be assigned to the vanishing of the electronic friction channel. The smooth friction reduction curve is in excellent agreement with expectations from superconductor theory (*29*), where a continuously decreasing number of unpaired electrons can still contribute to electronic friction even below T_c. Both the temperature and the velocity dependence of friction can be described by a superposition of friction contributions following the thermally activated PT model and an electronic friction channel, while noncontact phononic friction plays no significant role.

RESULTS AND DISCUSSION

To analyze the different contributions to the total sliding friction and the transition regime below T_c, we chose a BSCCO superconductor as model system. BSCCO is a layered van der Waals material and a well-known high-T_c superconductor with a generalized chemical formula of $Bi_2Sr_2Ca_{n-1}Cu_nO_{2n+4+x}$. Here, the critical superconducting transition temperature is typically elevated if the number of CuO_2 planes intermediated by Ca atoms increases. In our experiments, we used a crystal with $n = 2$ (purchased from 2D Semiconductors, USA), usually referred to as Bi-2212, with a critical transition temperature of T_c = 95 K. Clean and atomically flat sample surfaces suitable for analysis under ultrahigh vacuum (UHV) conditions were prepared by standard mechanical exfoliation techniques.

All single-asperity friction measurements have been performed by conventional FFM using standard silicon cantilevers in a UHV atomic force microscopy (AFM) system equipped with a temperature-controlled sample support cooled by liquid helium (Fig. 1A). To exclude any influence of varying surface roughness, we closely monitored the topography of the sample throughout our measurements. No difference in topography was noticed for measurements above and below the superconducting transition (see Fig. 1, B and C), but instead, atomically flat surfaces were found at each temperature. Since, additionally, the surface roughness is much lower than the tip diameter (~10 nm), we can conclude that the friction force is insensitive to the exact position of the tip on the BSCCO surface. During our experiments, we have also repeatedly measured the adhesion forces between the tip and the BSCCO sample. No changes of adhesion in relation to the superconducting phase transition have been found (see the Supplementary Materials).

In our experiments, systematic measurements have been performed for 15 different temperatures between 40 and 300 K. In each case, we cooled the sample to a fixed temperature and waited for at least 1.5 hours until thermal equilibrium was reached. After that, we measured the interfacial friction between the AFM tip and the BSCCO sample for different normal forces ranging from 6 to 38 nN. Figure 2 shows the average sliding friction as a function of temperature and normal load. Around the superconducting phase transition temperature of T_c = 95 K, we find a strong discontinuity ΔF_T in the

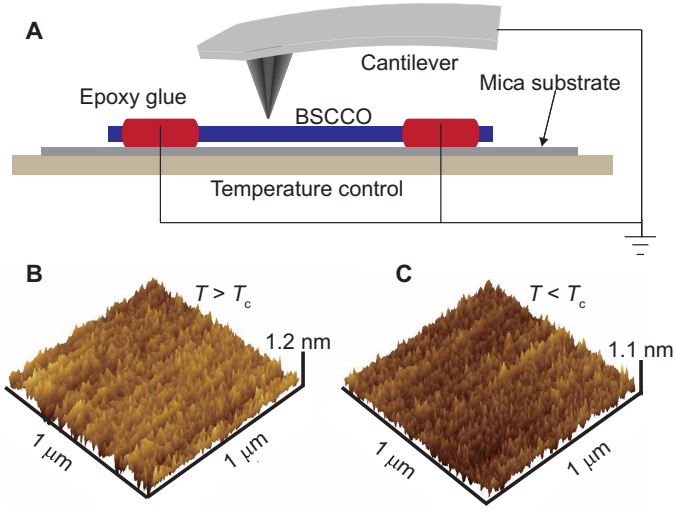

Fig. 1. Experimental setup and topography images of the BSCCO superconductor surface. (**A**) All experiments have been performed under UHV conditions using conventional FFM on a freshly cleaved BSCCO sample, which was in contact with the temperature control stage of the AFM. In addition, (**B**) and (**C**) show topography scans of the sample surface obtained at T = 104.1 and 79.7 K, i.e., above and below the transition temperature T_c, obtained in contact mode operation at a normal force of 14 nN and a scan velocity of 1 μm/s. In both cases, we find that the surfaces are atomically flat with no apparent differences between the two images, from which surface roughness values R_a of 0.094 ± 0.002 nm (T = 104.1 K) and 0.088 ± 0.005 nm (T = 79.7 K) can be calculated. In addition, the correlation length in the normal state is 12 ± 4 and 15 ± 8 nm in the superconducting state.

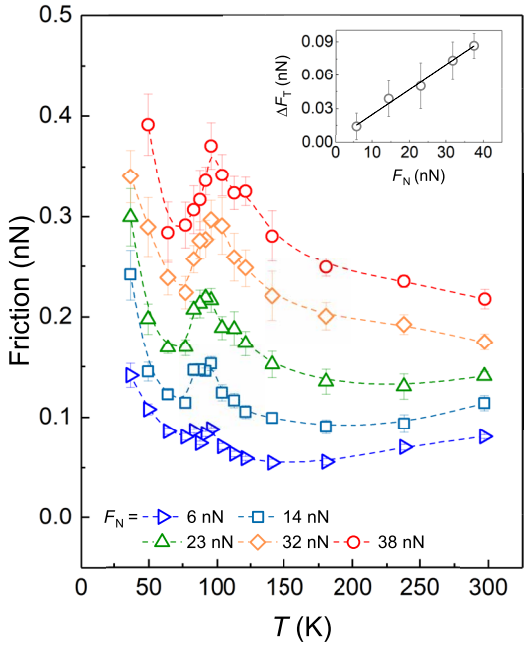

Fig. 2. Load and temperature dependence of nanoscale friction on BSCCO. Friction between the AFM tip and the BSCCO surface measured for five different loads between 6 and 38 nN as a function of temperature. For each temperature-dependent curve, a drop in friction was observed once the sample was cooled below T_c = 95 K. By quantifying this drop in friction as the difference ΔF_T between the local minima and maxima around T_c, we find a linear dependence of ΔF_T as a function of load (inset).

friction curves. This change in friction is measured as the difference between the local minimum and maximum of each curve around T_c. The inset of Fig. 2 shows ΔF_T as a function of load, indicating a linear dependence.

To quantify the friction coefficient, which is less influenced by possible tip changes and/or adhesion effects, we performed linear fits of the friction versus load curve for each temperature (Fig. 3A). We find no significant deviations from the linear approximation. The resulting friction coefficients are plotted against the temperature in Fig. 3B, ranging from 0.004 to 0.009. Those values are comparable to single-asperity sliding friction coefficients on other layered materials like, e.g., graphite, MoS_2, or h-BN (*30*–*32*). At this point, the overall friction and the friction drop ΔF_T both scale linear with load. This indicates that all friction channels scale similar with load, which is usually directly linked to the effective contact area.

Let us now assume that the two main contributions to low-wear nanoscale sliding friction are phononic and electronic friction channels. The phononic friction channel can again be subdivided in the noncontact and contact friction contribution. Previous investigations have focused on noncontact energy dissipation (*25*, *33*). In that case, electronic friction contributions can be identified by their characteristic dependence on the inverse tip sample distance d (*25*, *34*), and the phononic contributions, which are induced by elastic stress related to van der Waals forces between tip and sample, are expected to scale proportional to d^{-4}. For phononic noncontact friction, no explicit temperature dependence was found.

In contrast, for single-asperity sliding friction in contact the PT model has been extensively and successfully used to describe the temperature and velocity dependence (*6*, *10*, *35*, *36*). This model is based on the assumption that sliding friction is the average of successive stick-slip phases that are thermally activated. Temperature helps to overcome the energy barrier in the stick phases, and friction will decrease with temperature and increase logarithmically with velocity. Even if stick-slip, as in our case, is not explicitly resolved or does not even form as regular movement with atom-by-atom periodicity of the slips, this concept has proven to be a good description of temperature-dependent nanoscale friction. In a first approach, we now assume a linear superposition of this energy dissipation mechanism and an independent electronic friction channel. Furthermore, the previously investigated noncontact friction channels (*25*) are expected not to play a significant role for contact friction experiments with their generally higher interaction strength. On the basis of this premise, the solid blue line in Fig. 3B shows the fitting results to our friction data above T_c based on the PT model and including a constant offset to accommodate electronic friction effects (see also Materials and Methods). Below T_c, the gray dashed line represents the same phononic friction contribution without the constant offset. We conclude that this change in friction of approximately 30% around T_c is due to the onset of electronic friction effects, which are suppressed if the sample is in the superconducting state.

For a better analysis of the electronic friction branch, we substract the PT model fit curve (Fig. 3B, gray dashed line) from the total friction values. What remains is the electronic friction contribution as a function of temperature (Fig. 4). Models predict that the electronic friction does not necessarily vanish abruptly upon cooling the sample below T_c but can rather show a smooth transition following an exponential law (*7*, *12*). This transition law describes how the ratio of normal-state electrons to cooper pairs develops as a function of temperature below T_c, with friction originating from tip-driven excitation of the normal-state electrons in the surface layers, despite the overall resistance of the sample already being zero.

So far, only a few experiments have analyzed the energy dissipation process across the superconducting phase transition. For noncontact friction experiments, a smooth transition in accordance with these theoretical predictions was claimed before (*25*). Initial sliding friction experiments on a QCM first suggested an abrupt change of friction within some millikelvin (*19*), while later on, experiments of sliding adsorbate layers under optimized cryogenic conditions (*23*) support the concept of a smooth transition. FFM using magnetized metal–coated tips on a YBCO superconductor revealed a temperature dependence of the interfacial friction, which closely resembled the general shape of the temperature-dependent electrical resistivity (*16*).

Our results as shown in Fig. 4 unequivocally confirm the anticipated smooth transition for single-asperity contact friction. For a

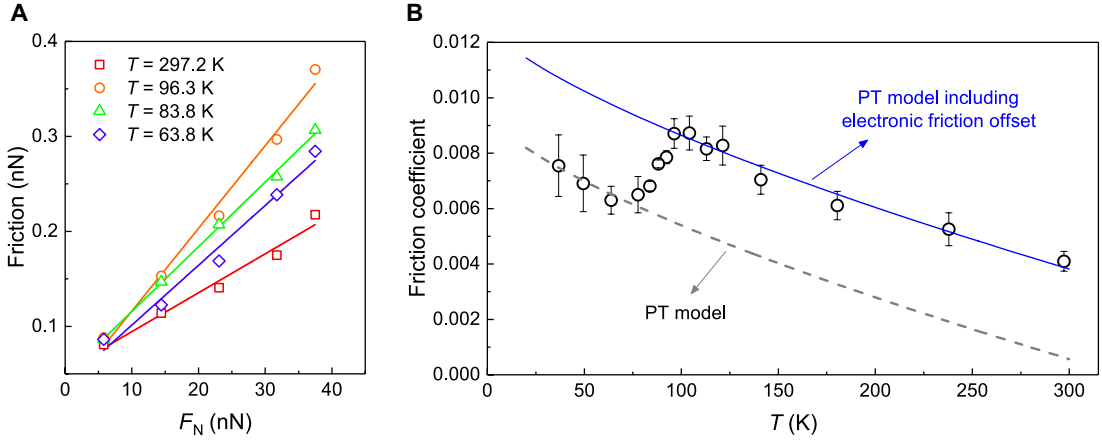

Fig. 3. Evaluation of friction coefficients and their temperature dependence. (**A**) Nanoscale friction on BSCCO as a function of normal force for a number of representative temperatures. Each normal force dependence can be fitted linearly in which case the slope equals the respective friction coefficient. (**B**) Temperature dependence of the friction coefficient (black circles). Again, a clear drop of the friction coefficients can be observed below T_c. For temperatures above T_c or well below T_c, the temperature-dependent friction coefficient is in good agreement to theoretical curves based on the thermally activated PT model, where a constant offset related to electronic friction is either considered (blue solid line) or not considered (gray dashed line).

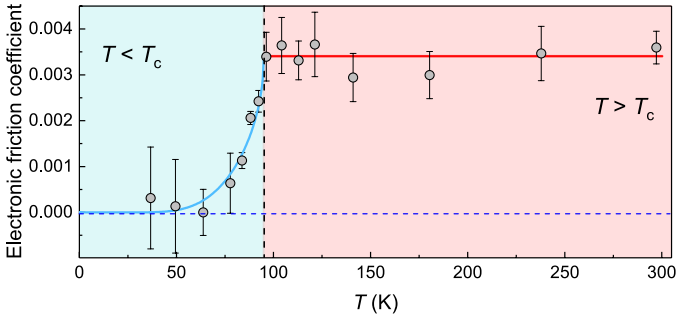

Fig. 4. Temperature dependence of electronic friction. The black circles show the friction coefficient representative for the electronic friction component both in the normal conducting state ($T > T_c$) and in the superconducting state ($T < T_c$). While the friction coefficient can be described by a constant value above T_c (red line), a gradual decrease can be observed for temperatures below T_c. Here, the friction coefficient is fitted by a model describing the remaining amount of conventional electrons as a function of temperature (cyan line).

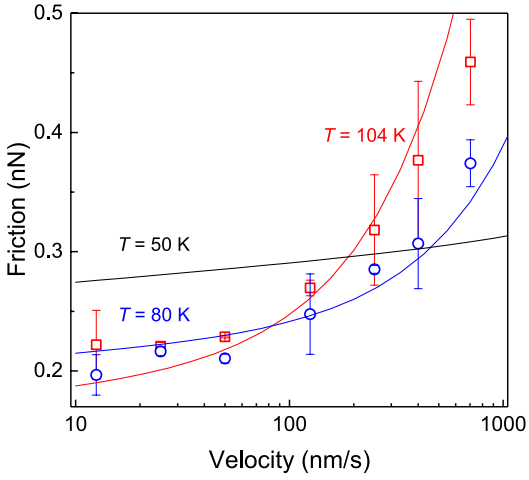

Fig. 5. Velocity dependence of friction above and below the superconducting phase transition. The red squares and blue circles show absolute friction values recorded for a normal force of $F_N = 14$ nN as a function of sliding velocity at $T = 104$ and 80 K, i.e., in the normal conducting state and in the superconducting state. The red, blue, and black lines represent the theoretical results at temperature 104, 80, and 50 K, respectively, obtained as a linear superposition of phononic and electronic friction contributions.

Bardeen-Cooper-Schrieffer (BCS) superconductor, the electronic friction caused by electron-phonon interaction follows the relation (*12*, *29*, *25*)

$$\frac{\mu(T)}{\mu(T_c)} = \frac{2}{e^{(\Delta(T)/k_B T)} + 1} \quad (1)$$

The temperature dependence of the energy bandgap $\Delta(T)$ can be expressed by $\Delta(T)/\Delta_0 = 1.74(1 - T/T_c)^{1/2}$ (*37*), where Δ_0 is the energy gap at $T = 0$ K, which can be calculated by $\Delta_0 = (C/2)k_B T_c$, with typically $C = 3.5$ for traditional BCS superconductors. For high-temperature copper oxide superconductors, higher values of C are expected, typically ranging from 4 to 8 for BSCCO to account for the specific pair-breaking scattering and strong coupling (*38*, *39*). The cyan line in Fig. 4 shows a fit to the friction model based on Eq. 1 with $C = 4.4 \pm 0.2$, exhibiting a good agreement between experiment and theory.

Another aspect of the two friction channels is their different characteristic dependence on the sliding velocity. While the PT model predicts a logarithmic increase in friction with velocity, a frequent approach for electronic friction contributions is to assume a linear scaling with the sliding velocity, e.g., as a result of the viscous drift motion of the normal electrons in a two-fluid model for superconductors (*12*). Figure 5 shows the velocity dependence of friction measured for two characteristic temperatures $T = 80$ and 104 K, below and above T_c, respectively. The solid lines show predicted friction versus velocity curves for three temperatures around T_c, calculated as a linear superposition of the PT model and the BCS theory–based electronic friction component. All parameters for the theoretical curves are taken from the fits of the PT model in Fig. 3, thereby also preserving the relative ratio of the friction contributions at $v_0 = 250$ nm/s. The only addition is a constant factor that is required to link the previously analyzed friction coefficients to absolute lateral force values recorded during the velocity-dependent measurements (see Materials and Methods for more details). As expected, the low-velocity values are dominated by the friction branch related to the PT model, while at higher velocities, friction values are dominated by the electronic friction branch. Both curves at 80 and 104 K show a much faster increase in friction with velocity as would be expected on the basis of the conventional PT model alone (cf. theoretical curve at 50 K).

From Figs. 4 and 5, several conclusions can be drawn. We find that our sliding friction experiments of a nanoscale contact on BSCCO can well be described as a linear superposition of contact friction based on the thermally activated PT model and an independent electronic friction channel. In this context, we find that the model developed by Persson (*12*), which describes energy dissipation by drag effects on the remaining normal-state electrons in the surface layers of a superconductor, fits well to the temperature-dependent friction changes below T_c.

Still, it is not clear how such a mechanism can be reconciled with the absolute friction changes observed in our experiments. In general, ohmic losses related to electron-hole pair creation or adsorbate-induced scattering are often considered as mechanisms to describe the role of electrons in the energy dissipation process during sliding (*13*, *14*), but estimations for point contact friction on semiconductors (*15*) and YBCO superconductors (*16*) suggest that these ohmic contributions are generally too low by several orders of magnitude. Only for the case of nitrogen adsorbates sliding on lead in QCM experiments (*19*) could the magnitude of friction changes be reconciled with ohmic losses originating from interaction with the electrostatic moments of the adsorbates (*40*).

Alternatively, charge trapping mechanisms have been proposed to explain electronic friction effects (*15*, *16*). Here, charges are supposed to be injected into a surface layer during scanning with subsequent electrostatic interaction between these charges and the AFM tip, which was successfully applied to friction phenomena on semiconductors (*1*, *15*). In addition, for nanofriction on cuprate superconductors, this mechanism was applied to explain experimental findings; however, a semiconducting top layer of the superconductor is required (*41*, *42*). Last but not least, electron-phonon coupling may play an important role, which is believed to be a major mechanism for ultrasound attenuation in superconductors (*29*, *43*). In our nanofriction experiments, a decreasing number of normal-state electrons below T_c could slow down the attenuation of lattice vibrations generated during the sliding process. Marked changes in friction forces were recently explained in the context of different electron-phonon coupling

strength on single-layer versus double-layer graphene (*17*). However, detailed theoretical investigations would be necessary to solidify this hypothesis.

CONCLUSIONS

Our experiments unambiguously link electronic friction effects to the number of normal-state electrons in the superconducting phase below T_c, allowing us to estimate the relative importance of the electron system to overall friction.At around 100 K, the electron-related friction contribution represents 30% of the total sliding friction signal. However, at higher velocities and higher temperature, it can even dominate the total friction, as was found for $T = 104$ K and $v = 800$ nm/s, where the electronic friction exceeds 50% of the total friction signal. Although these ratios can sensitively depend on the exact tip configuration, our experiments demonstrate that electronic friction must explicitly be taken into account in models describing single-asperity sliding friction and probably also plays a more important role than so far anticipated for larger multiasperity tribocontacts. Electronic friction may also be an important factor for recent emerging applications of superlubricity (*28*), which relies on vanishing potential energy barriers for sliding.

MATERIALS AND METHODS

Experimental methods

In our experiments, we used a commercial BSCCO sample of square size with a width of 5 mm and a thickness of 2 mm. Two opposite points of this sample were glued onto a mica substrate using of conductive epoxy glue (Epoxy Technology, USA), and then, the mica substrate was mechanically fixed to a standard Omicron low-temperature sample holder. The sample holder was coupled to a flow cryostat using liquid helium as coolant (see also Fig. 1A). Adjusting both the flow of liquid helium and the heating power of a resistor integrated to the cooling stage allowed varying the temperature of the sample approximately in a range of 30 to 300 K. The BSCCO was freshly cleaved by scotch tape directly before transfer into the UHV chamber. Inside the UHV chamber, the BSCCO was additionally heated up to 550 K for 10 hours to remove residual adsorption from the surface and prepare a clean sample surface for the tribological analysis. All experiments have been performed within an Omicron UHV variable temperature scanning probe microscope using PointProbe Plus Lateral Force Microscopy - Reflex Coating (PPP-LFMR) cantilevers obtained from Nanosensors (Switzerland) with a nominal normal force constant of $k = 0.65$ N/m and a typical tip diameter of 10 nm. During our measurements, an average pressure of about 3×10^{-10} mbar was constantly maintained. All measurements have been performed in contact mode operation with normal forces as specified in the Results and Discussion section. After bringing the tip into contact with the cooled sample surface, we typically waited for several minutes. During this time, a thermal equilibrium between tip and sample is established. The fact that our experiments accurately reproduced the superconducting transition temperature expected for this material confirms that the temperature at the interface does not differ significantly from the undisturbed sample temperature. We used a scanning area of 50 nm by 50 nm for all friction measurements. If not specified otherwise, the scanning velocity was fixed to $v = 250$ nm/s. To obtain sufficient statistics, we used the up-down scanning mode, and each data point was extracted from the lateral force signals of six images. All lateral force values have been calibrated using the approach suggested by Bilas *et al.* (*44*). The error bars in Fig. 2 are based on the SEM value calculated from the six images measured for each temperature and normal load.

Theoretical approach

In our experiments, we found that friction always scales linear with the applied normal force. As a consequence, the friction coefficients μ_{ph} and μ_{el} have been defined. To describe μ_{ph}, we then used an analogy to the well-established velocity and temperature dependence of the thermally activated PT model as described by Sang *et al.* (*45*). In addition, the electronic friction has been introduced as a constant offset μ_{el}, which vanishes well below the phase transition temperature T_c. On the basis of this model, the relation between friction coefficient, temperature, and velocity above T_c can be written as

$$\mu(v,T) = \mu_{ph} + \mu_{el} = \left[\alpha - \beta T^{2/3}\left(\ln\left(\gamma\frac{T}{v}\right)\right)^{2/3}\right] + \mu_{el}$$

This model with fit parameters α, β, and γ can be used to explain the experimental data above the superconducting transition, while μ_{el} can at the same time be extracted from the discontinuity of the friction coefficient below the phase transition temperature. The resulting fit parameters are $\alpha = 0.0095$, $\beta = 3.10 \times 10^{-5}$ $N^{3/2}m^{-1}$, and $\gamma = 0.0097$ $(m \cdot Hz/K)^{3/2}$. The solid blue line and the gray dashed line of Fig. 3B then represent the phononic friction contribution with or without the electronic friction offset of $\mu_{el} = 0.0032$.

On the basis of the PT model and a linear dependence of the electronic friction component on velocity, the combined temperature and velocity dependence of the total friction can be written as

$$F(v,T) = \delta \times F_N \times \left[\left(\alpha - \beta T^{2/3}\left(\ln\left(\gamma\frac{T}{v}\right)\right)^{2/3}\right) + \frac{v}{v_0} \times \mu_{el} \times \psi(T)\right]$$

$$\psi(T) = \begin{cases} \dfrac{2}{e^{(\Delta(T)/k_B T)} + 1} & T \le T_c \\ 1 & T > T_c \end{cases}$$

where $\psi(T)$ defines the change of electronic friction coefficient by BCS theory, $v_0 = 250$ nm/s is the reference velocity, $F_N = 14$ nN is the normal force, and $\mu_{el} = 0.0032$ represents the contribution of electronic friction for $T > T_c$. By substituting the previously obtained parameters and introducing a parameter $\delta = 2.7$ to account for tip changes, we can reproduce the effects of velocity on friction (Fig. 5).

SUPPLEMENTARY MATERIALS

Supplementary material for this article is available at http://advances.sciencemag.org/cgi/content/full/6/12/eaay0165/DC1

Section S1. Fit to the total friction coefficient
Section S2. Independent control experiments
Section S3. Heating result
Section S4. Temperature dependence of adhesion effects
Table S1. Fitting parameter values in Eq. 1.
Fig. S1. Temperature dependence of friction coefficient.
Fig. S2. Load and temperature dependence of nanoscale friction on BSCCO.
Fig. S3. Temperature dependence of nanoscale friction on BSCCO measured upon heating the sample from 70 to 112 K with a constant normal load of $F_N = 14$ nN.
Fig. S4. Temperature dependence of nanoscale adhesion forces between the AFM tip and BSCCO measured for two sets of experiments.

REFERENCES AND NOTES

1. J. Y. Park, M. Salmeron, Fundamental aspects of energy dissipation in friction. *Chem. Rev.* **114**, 677–711 (2014).
2. M. H. Müser, M. Urbakh, M. O. Robbins, Statistical mechanics of static and low-velocity kinetic friction, in *Advances in Chemical Physics*, I. Prigogine, S. A. Rice, Eds. (John Wiley & Sons Inc., 2003), pp. 187–272.

3. I. Svetlizky, J. Fineberg, Classical shear cracks drive the onset of dry frictional motion. *Nature* **509**, 205–208 (2014).
4. E. Gnecco, E. Meyer, Nanoscience and technology, in *Fundamentals of Friction and Wear on the Nanoscale*, (Springer, ed. 2, 2015).
5. Y. Mo, K. T. Turner, I. Szlufarska, Friction laws at the nanoscale. *Nature* **457**, 1116–1119 (2009).
6. L. Jansen, H. Hölscher, H. Fuchs, A. Schirmeisen, Temperature dependence of atomic-scale stick-slip friction. *Phys. Rev. Lett.* **104**, 256101 (2010).
7. B. N. J. Persson, E. Tosatti, The puzzling collapse of electronic sliding friction on a superconductor surface. *Surf. Sci.* **411**, L855–L857 (1998).
8. Y. Mo, M. H. Müser, I. Szlufarska, Origin of the isotope effect on solid friction. *Phys. Rev. B* **80**, 155438 (2009).
9. L. Prandtl, Ein Gedankenmodell zur kinetischen Theorie der festen Körper. *Zeitschrift für Angewandte Mathematik und Mechanik* **8**, 85–106 (1928).
10. E. Gnecco, R. Bennewitz, T. Gyalog, C. Loppacher, M. Bammerlin, E. Meyer, H.-J. Güntherodt, Velocity dependence of atomic friction. *Phys. Rev. Lett.* **84**, 1172–1175 (2000).
11. U. D. Schwarz, H. Hölscher, Exploring and explaining friction with the Prandtl–Tomlinson model. *ACS Nano* **10**, 38–41 (2016).
12. B. N. J. Persson, Electronic friction on a superconductor surface. *Solid State Commun.* **115**, 145–148 (2000).
13. T. Novotný, B. Velický, Electronic sliding friction of atoms physisorbed at superconductor surface. *Phys. Rev. Lett.* **83**, 4112–4115 (1999).
14. J. B. Sokoloff, M. S. Tomassone, A. Widom, Strongly temperature dependent sliding friction for a superconducting interface. *Phys. Rev. Lett.* **84**, 515–517 (2000).
15. Y. Qi, J. Y. Park, B. L. M. Hendriksen, D. F. Ogletree, M. Salmeron, Electronic contribution to friction on GaAs: An atomic force microscope study. *Phys. Rev. B* **77**, (2008).
16. I. Altfeder, J. Krim, Temperature dependence of nanoscale friction for Fe on YBCO. *J. Appl. Phys.* **111**, 094916 (2012).
17. T. Filleter, J. L. McChesney, A. Bostwick, E. Rotenberg, K. V. Emtsev, T. Seyller, K. Horn, R. Bennewitz, Friction and dissipation in epitaxial graphene films. *Phys. Rev. Lett.* **102**, 086102 (2009).
18. S. Y. Krylov, J. W. M. Frenken, The physics of atomic-scale friction: Basic considerations and open questions. *Phys. Status Solidi B* **251**, 711–736 (2014).
19. A. Dayo, W. Alnasrallah, J. Krim, Superconductivity-dependent sliding friction. *Phys. Rev. Lett.* **80**, 1690–1693 (1998).
20. M. Highland, J. Krim, Superconductivity dependent friction of water, nitrogen, and superheated he films adsorbed on Pb(111). *Phys. Rev. Lett.* **96**, 226107 (2006).
21. M. Pierno, L. Bruschi, G. Mistura, C. Boragno, F. B. de Mongeot, U. Valbusa, C. Martella, Nanofriction of adsorbed monolayers on superconducting lead. *Phys. Rev. B* **84**, 035448 (2011).
22. R. L. Renner, P. Taborek, J. E. Rutledge, Friction and pinning of nitrogen films on lead substrates near the superconducting transition. *Phys. Rev. B* **63**, 233405 (2001).
23. B. L. Mason, S. M. Winder, J. Krim, On the current status of quartz crystal microbalance studies of superconductivity-dependent sliding friction. *Tribol. Lett.* **10**, 59–65 (2001).
24. J. Y. Park, D. F. Ogletree, P. A. Thiel, M. Salmeron, Electronic control of friction in silicon pn junctions. *Science* **313**, 186–186 (2006).
25. M. Kisiel, E. Gnecco, U. Gysin, L. Marot, S. Rast, E. Meyer, Suppression of electronic friction on Nb films in the superconducting state. *Nat. Mater.* **10**, 119–122 (2011).
26. Y. Fang, S. Danyluk, M. T. Lanagan, K. C. Goretta, Effect of temperature on the coefficient of friction of $Bi_2Sr_2CaCu_2O_x$/$Bi_2Sr_2CaCu_2O_x$ and $Bi_2Sr_2CaCu_2O_x$/Ag. *J. Mater. Sci. Lett.* **13**, 852–855 (1994).
27. Q. Ding, C. Li, L. Dong, M. Wang, Y. Peng, Y. Xuehua, Preparation and properties of $YBa_2Cu_3O_{7-\delta}$/Ag self-lubricating composites. *Wear* **265**, 1136–1141 (2008).
28. M. Z. Baykara, M. R. Vazirisereshk, A. Martini, Emerging superlubricity: A review of the state of the art and perspectives on future research. *Appl. Phys. Rev.* **5**, 041102 (2018).
29. J. Bardeen, L. N. Cooper, J. R. Schrieffer, Theory of superconductivity. *Phys. Rev.* **108**, 1175–1204 (1957).
30. J.-A. Ruan, B. Bhushan, Atomic-scale and microscale friction studies of graphite and diamond using friction force microscopy. *J. Appl. Phys.* **76**, 5022–5035 (1994).
31. K. Miura, S. Kamiya, Observation of the amontons-coulomb law on the nanoscale: Frictional forces between MoS_2 flakes and MoS_2 surfaces. *EPL Europhys. Lett.* **58**, 610 (2002).
32. Y. Liu, A. Song, Z. Xu, R. Zong, J. Zhang, W. Yang, R. Wang, Y. Hu, J. Luo, T. Ma, Interlayer friction and superlubricity in single-crystalline contact enabled by two-dimensional flake-wrapped atomic force microscope tips. *ACS Nano* **12**, 7638–7646 (2018).
33. B. C. Stipe, H. J. Mamin, T. D. Stowe, T. W. Kenny, D. Rugar, Noncontact friction and force fluctuations between closely spaced bodies. *Phys. Rev. Lett.* **87**, 096801 (2001).
34. A. I. Volokitin, B. N. J. Persson, H. Ueba, Giant enhancement of noncontact friction between closely spaced bodies by dielectric films and two-dimensional systems. *J. Exp. Theor. Phys.* **104**, 96–110 (2007).
35. M. H. Müser, Velocity dependence of kinetic friction in the Prandtl-Tomlinson model. *Phys. Rev. B* **84**, 125419 (2011).
36. C. Fusco, A. Fasolino, Velocity dependence of atomic-scale friction: A comparative study of the one- and two-dimensional tomlinson model. *Phys. Rev. B* **71**, 045413 (2005).
37. L. Coffey, Comment on "spin dynamics at oxygen sites in $YBa_2Cu_3O_7$". *Phys. Rev. Lett.* **64**, 1071 (1990).
38. Y. Li, J. Liu, C. M. Lieber, Dependence of the energy gap on T_c: Absence of scaling in the copper oxide superconductors. *Phys. Rev. Lett.* **70**, 3494–3497 (1993).
39. Y. Huang, Y. Wang, Z. Zhao, Internal friction and ultrasonic attenuation related to carriers in high-T_c superconductors. *Phys. Rev. B* **49**, 1320 (1994).
40. L. W. Bruch, Ohmic damping of center-of-mass oscillations of a molecular monolayer. *Phys. Rev. B* **61**, 16201–16206 (2000).
41. W. Groen, D. de Leeuw, Oxygen content, lattice constants and T_c of $Bi_2Sr_2CaCu_2O_{8+\delta}$. *Physica C Supercond.* **159**, 417–421 (1989).
42. N. Tulina, I. Y. Borisenko, V. Sirotkin, Bipolar resistive switchings in $Bi_2Sr_2CaCu_2O_{8+\delta}$. *Solid State Commun.* **170**, 48–52 (2013).
43. R. W. Morse, P. Tamarkin, H. Bohm, Ultrasonic attenuation in superconducting indium. *Phys. Rev.* **101**, 1610–1611 (1956).
44. P. Bilas, L. Romana, B. Kraus, Y. Bercion, J. L. Mansot, Quantitative characterization of friction coefficient using lateral force microscope in the wearless regime. *Rev. Sci. Instrum.* **75**, 415–421 (2004).
45. Y. Sang, M. Dubé, M. Grant, Thermal effects on atomic friction. *Phys. Rev. Lett.* **87**, 174301 (2001).

Acknowledgments

Funding: D.D. and A.S. thank for financial support provided by the German Research Foundation (projects DI917/7-1 and SCHI619/10-1). W.W. acknowledges funding from the Alexander von Humboldt Foundation, the financial support by the NSFC (grant nos. 11602205 and 11890672), and the Fundamental Research Funds for the Central Universities (grant nos. 2682018CX11 and 2682016ZY03). **Author contributions:** A.S. conceived the study. All authors designed the experiment(s). W.W. conducted the experiment(s). W.W. and D.D. analyzed the results. All authors discussed the results and contributed to writing the manuscript. **Competing interests:** The authors declare that they have no competing interests. **Data and materials availability:** All data needed to evaluate the conclusions in the paper are present in the paper and/or the Supplementary Materials. Additional data related to this paper may be requested from the authors.

Submitted 13 May 2019
Accepted 20 December 2019
Published 20 March 2020
10.1126/sciadv.aay0165

Citation: W. Wang, D. Dietzel, A. Schirmeisen, Single-asperity sliding friction across the superconducting phase transition. *Sci. Adv.* **6**, eaay0165 (2020).

ScienceAdvances

Single-asperity sliding friction across the superconducting phase transition

Wen WangDirk DietzelAndré Schirmeisen

Sci. Adv., 6 (12), eaay0165. • DOI: 10.1126/sciadv.aay0165

Science Advances (ISSN 2375-2548) is published by the American Association for the Advancement of Science. 1200 New York Avenue NW, Washington, DC 20005. The title *Science Advances* is a registered trademark of AAAS.